

FuseDream: Training-Free Text-to-Image Generation with Improved CLIP+GAN Space Optimization

Xingchao Liu¹, Chengyue Gong¹, Lemeng Wu¹, Shujian Zhang¹, Hao Su², Qiang Liu¹

¹University of Texas at Austin, ²University of California, San Diego

{xcliu, szhang19}@utexas.edu, haosu@eng.ucsd.edu, {cygong, lmwu, lqiang}@cs.utexas.edu



Figure 1. Generated images for three query texts about dogs with different methods, including naive optimization with CLIP+GAN (top left of each panel), BigSleep [20] (top right of each panel), and FuseDream (the bottom row) with BigGAN-256 (left) and 512 (right).

Abstract

Generating images from natural language instructions is an intriguing yet highly challenging task. We approach text-to-image generation with a CLIP+GAN approach, which optimizes in the latent space of an off-the-shelf GAN to find images that achieve maximum semantic relevance score with the given input text as measured by the CLIP model. Compared to traditional methods that train generative models mapping from text to image starting from scratch, the CLIP+GAN approach is training-free, zero-shot and can be easily customized with different generators.

However, optimizing CLIP score in the GAN space casts a highly challenging optimization problem and off-the-shelf optimizers such as Adam fail to yield satisfying results. In this work, we propose a FuseDream pipeline, which improves the CLIP+GAN approach with three key techniques: 1) a AugCLIP score which robustifies the standard CLIP score by introducing random augmentation on image. 2) a novel initialization and over-parameterization strategy for optimization which allows us to efficiently navigate the non-convex landscape in GAN space. 3) a composed generation technique which, by leveraging a novel bi-level optimization formulation, can compose multiple images to extend the GAN space and overcome the data-bias.

When promoted by different input text, FuseDream can

generate high-quality images with varying objects, backgrounds, artistic styles, and novel counterfactual concepts that do not appear in the training data of the GAN that we use. Quantitatively, the images generated by FuseDream yield top-level Inception score and FID score on MS COCO dataset, without additional architecture design or training. Our code is publicly available at <https://github.com/gnabitab/FuseDream>.

1. Introduction

A landmark task in multi-modal machine learning is text-to-image generation, generating realistic images that are semantically related to a given text input [9, 18, 25, 26, 31, 35]. This is a highly challenging task because the generative model needs to understand the text, image, and how they should be associated semantically. Recently, significant progresses have been achieved by [9, 25] which generate high quality and semantically relevant images using models trained with self-supervised loss on large-scale datasets.

The traditional approach to text-to-image generation is to train a conditional generative model from scratch with a dataset of (text, image) pairs [18, 22, 25, 26, 31, 35]. This procedure, however, requires to collect a large training dataset, casts a high training cost, and can not be easily

customized. Recently, a more flexible text-to-image generation approach is enabled with the availability of powerful joint text-image encoders (notably the CLIP model [24]) that provide faithful semantic relevance score of text-image pairs. Together with powerful pre-trained GANs (such as [1, 4, 18, 40]), it is made possible to do text-to-image generation by optimizing in the latent space of a GAN to create images that have high semantic relevance with the input text. Notable examples include BigSleep [20] and VQ-GAN+CLIP [6], which can generate intriguing and artistic images from text by maximizing the CLIP score in the latent space of BigGAN and VQGAN, respectively. Compared with the traditional benchmarks, methods that combine GAN and CLIP are training-free and zero-shot, requiring no dedicated training dataset and training cost. It is also much more flexible and modular: a user can easily replace the generator (GAN) or the encoder model (CLIP) with more powerful or customized ones that fit best for their own problems and computational budget.

On the other hand, the results from the existing CLIP+GAN methods [6, 10, 20] are still not satisfying in many cases. For example, although BigSleep can generate images in different styles and create interesting visual arts, it finds difficulty in generating clear and realistic images and the resulting images can be only weakly related to the query text. As shown in Figure 1 (top right of each panel), BigSleep can not generate a clearly recognizable image for the simple concept of ‘blue dog’. For counterfactual concepts like ‘flaming dog’, the image given by BigSleep tends to entangle the flame and dog concepts in an unnatural way. In Figure 1 (top left of each panel), we implement another baseline that maximizes the CLIP score in the input space of BigGAN [4] with the off-the-shelf Adam [17] optimizer, which yields even worse results than BigSleep.

In this work, we analyze the problems in the existing CLIP+GAN procedures. We identify three key bottlenecks of the exiting approach and address them with a number of techniques to significantly improve the pipeline.

1) Robust Score We observe that the original CLIP score does not serve as a good objective function for optimizing in the GAN space, as it tends to yield semantically unrelated images that “adversarially” maximize the CLIP score. We propose an AugCLIP score, which robustifies the CLIP score by averaging it on multiple perturbation or augmentation of the input images.

2) Improved Optimization Strategy Maximizing the CLIP score in the GAN space yields a highly non-convex, multi-modal optimization problem and off-the-shelf optimization methods tend to be stuck at sub-optimal local maxima. We address this problem with a novel initialization and over-parameterization strategy which allow us to traverse in the non-convex loss landscape more efficiently.

3) Composed Generation The image space of the CLIP+GAN approach is limited by the pre-trained GAN that we use. This makes it difficult to generate images with novel combinations of objects that did not appear in the training data of the GAN. We address this problem by proposing a *composed generation* technique, which co-optimizes two images so that they can be seamless composed together to yield a natural and semantically relevant image. We formulate composed generation into a novel bi-level optimization problem, which maximizes AugCLIP score while incorporating a perceptual consistency score as the secondary objective, and solve it efficiently with a recent dynamic barrier gradient descent algorithm [11].

Our pipeline, which we call *FuseDream*¹, can generate not only clear objects from complex text description, but also complicate scenes as these in MS COCO [19]. Thanks to the representation power of CLIP, *FuseDream* can create images with different backgrounds, textures, locations, artistic styles, and even counterfactual objects. With the composed generation techniques, *FuseDream* can create images with novel combinations of objects that do not appear in original training data of the GAN that we use. Comparing to directly training large-scale text-to-image generative models, our method is much more computation-friendly while achieving comparable or even better results.

2. Text-to-Image Generation with CLIP+GAN

We first introduce the general idea of text-to-image generation by combining pre-trained image generators (in particular GANs) and joint image+text encoders (in particular CLIP). We then analyze a key limitation of the naive realization of this approach.

GAN An image generator $g: \mathbb{R}^D \rightarrow \mathbb{R}^{H \times W \times 3}$ is a neural network that takes an D -dimensional latent code ξ and output a colored image \mathcal{I} of size $H \times W$. Formally,

$$\mathcal{I} = g(\xi).$$

One can generate and manipulate different images by controlling the input ξ . In this work, we use BigGAN [4] unless otherwise specified, which is a class-conditional GAN whose latent vector $\xi = \{z, y\}$ includes both a Gaussian noise vector $z \in \mathbb{R}^Z$ and a class embedding vector $y \in \mathbb{R}^Y$. It was trained on the large-scale ImageNet dataset [27] with objects from 1,000 different categories.

CLIP A joint image-text encoder, notably *Contrastive Language-Image Pretraining* (CLIP) [24], consists of a pair of language encoder f_{text} and image encoder f_{image} , which map a text \mathcal{T} and an image \mathcal{I} into a common latent space on which their relevance can be evaluated by cosine similarity

$$s_{\text{CLIP}}(\mathcal{T}, \mathcal{I}) = \frac{\langle f_{\text{text}}(\mathcal{T}), f_{\text{image}}(\mathcal{I}) \rangle}{\|f_{\text{text}}(\mathcal{T})\| \cdot \|f_{\text{image}}(\mathcal{I})\|}. \quad (1)$$

¹The “fuse” in the name refers to both the idea of 1) fusing GAN and CLIP and 2) our composed generation technique.

The CLIP model was trained such that semantically related pairs of \mathcal{T} and \mathcal{I} have high similarity scores.

CLIP+GAN One can synthesis a text-to-image generator by combining a pre-trained GAN g and CLIP $\{f_{text}, f_{image}\}$. Given an input text \mathcal{T} , we can generate a realistic image \mathcal{I} that is semantically related to \mathcal{T} by optimizing the latent code ξ such that the generated image $\mathcal{I} = g(\xi)$ has maximum CLIP score $s_{CLIP}(\mathcal{T}, \mathcal{I})$. Formally,

$$\max_{\xi} s_{CLIP}(\mathcal{T}, g(\xi)). \quad (2)$$

This confines the output image within the space of natural images while maximizing the semantic relevance to the input text. The optimization is solved with Adam [17] in [20, 39]. We truncate z to $[-2, 2]$ as a typical practice when using BigGAN [4, 16].

2.1. CLIP Can be Easily Attacked and Stuck

Naively solving (2) does not yield satisfying images as shown in the top-left images of Figure 1. We observe that the unsatisfying results can be attributed to two interconnected reasons:

- 1) CLIP scores can be easily “attacked”, in that it is easy to maximize CLIP within a small neighborhood of any image, indicating the existence of “adversarial” images with high CLIP score but low semantic relevance with the input text.
- 2) The optimization in (2) can indeed effectively act as an adversarial optimization on s_{CLIP} , yielding images that are similar to the initialization but spuriously high CLIP score.

Case Study 1: Attacking CLIP As shown in Figure 2, we apply an adversarial attacker, Fast Gradient Sign Method (FGSM) [13] on s_{CLIP} on a natural image \mathcal{I} , that is, we solve $\max_{\delta} s_{CLIP}(\mathcal{I} + \delta)$ s.t. $\|\delta\| \leq \epsilon$ with a small perturbation magnitude $\epsilon > 0$. We find that FGSM can easily find an image that is almost identical with the original image, yet with much higher CLIP score. This indicates a danger of “overfitting” when we directly maximize the CLIP score.

Case Study 2: Dog→Cat In Figure 3, we show an example of optimizing (2) with an input text \mathcal{T} =‘A photo of a cat’, initialized from an ξ^0 whose image $\mathcal{I} = g(\xi^0)$ is a dog. We can see that although s_{CLIP} is successfully maximized, the image remains similar to the initialization and does not transfer from a dog to a cat as expected. In this case, the optimization in (2) exhibit an adversarial attack-like behavior: it is stuck nearby the initialization while spuriously increasing the CLIP score.

In both cases above, the problem can be resolved by using our AugCLIP score, which we introduce in sequel.

3. Our Method - FuseDream

We now introduce our main techniques for improving the CLIP+GAN pipeline. Section 3.1 introduces the AugCLIP

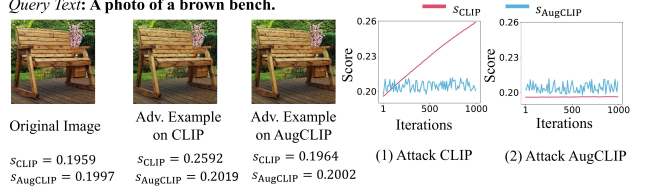


Figure 2. Results of adversarial attack on CLIP and AugCLIP score. (1) By applying FGSM on CLIP score, we get an image that has high s_{CLIP} but visually identical to the original image. (2) Our AugCLIP score is robust against the FGSM attacking.

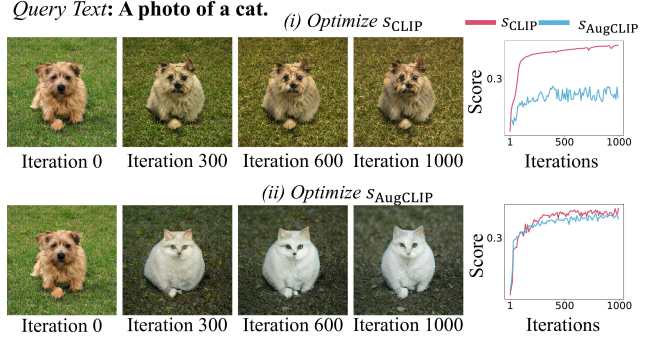


Figure 3. Optimizing s_{CLIP} and $s_{AugCLIP}$ in the GAN space as (2). Initialized from a dog image, maximizing s_{CLIP} only slightly changes in color of image while yielding spurious increase of s_{CLIP} (top row). But maximizing $s_{AugCLIP}$ quickly turns the dog into a white cat (bottom row). Note that maximizing $s_{AugCLIP}$ yields a similar amount of increase on s_{CLIP} , but not the other way around.

score which robustifies the CLIP score to avoid the adversarial attacking phenomenon. Section 3.2 introduces an initialization and over-parameterization technique to better solve the non-convex optimization. Section 3.3 introduces a *composed generation* to generate out-of-distribution images with novel combination of objects and backgrounds.

3.1. AugCLIP: Avoiding Adversarial Generation

To address the adversarial attacking issue of the CLIP score, we propose the following AugCLIP score,

$$s_{AugCLIP}(\mathcal{T}, \mathcal{I}) = \mathbb{E}_{\mathcal{I}' \sim \pi(\cdot|\mathcal{I})} [s_{CLIP}(\mathcal{T}, \mathcal{I}')], \quad (3)$$

where \mathcal{I}' is a random perturbation of the input image \mathcal{I} drawn from a distribution $\pi(\cdot|\mathcal{I})$ of candidate data augmentations. In our work, we adopt the various data augmentation techniques considered in DiffAugment [38], including random colorization, random translation, random resize, and random cutout.

AugCLIP is more robust against adversarial attacks, because a successful adversarial perturbation against AugCLIP must simultaneously attack s_{CLIP} on most of the randomly augmented images, which is much harder than attacking a single image. The averaging over random aug-

mentation also makes the landscape smoother and hence harder to attack, as shown theoretically and empirically in [5, 28]. Meanwhile, adding the augmentation does not hurt the semantic relation encoded by CLIP, because the CLIP model was originally trained on images with different colorizations, views and translations, and is hence compatible with our augmentation strategy.

Case Study 1 & 2 As shown in Figure 3, the s_{AugCLIP} score is significantly more robust against adversarial attacking. Figure 4 shows that simply replacing s_{CLIP} with s_{AugCLIP} allows us to escape the adversarial generation regime and yield more semantically relevant images.

3.2. Improving Optimization

The optimization of s_{AugCLIP} can still suffer from sub-optimal local maxima due to the high non-convexity of loss landscape. We introduce an initialization and over-parameterization strategy to improve the optimization.

Unlike traditional methods that start from a single initialization, we start with sampling a large number M of copies of initialization $\{\xi_i^0\}_{i=1}^M$. We then select the top k initialization, say $\{\xi_{(i)}^0\}_{i=1}^k$, that has the highest s_{AugCLIP} score, and use them as the *initial basis vector* for the subsequent optimization, that is, we reparameterize the solution into $\xi = \sum_{i=1}^k w_{(i)} \xi_{(i)}$ and jointly optimize the basis vectors $\{\xi_{(i)}\}_{i=1}^k$ and the coefficients $\{w_{(i)}\}_{i=1}^k$ with $w_{(i)} \in \mathbb{R}$:

$$\max_{\{\xi_{(i)}, w_{(i)}\}_{i=1}^k} s_{\text{AugCLIP}} \left(\mathcal{T}, g \left(\sum_{i=1}^k w_{(i)} \xi_{(i)} \right) \right), \quad (4)$$

with $\{\xi_{(i)}\}$ initialized from the k selected $\{\xi_{(i)}^0\}$, and $w_{(i)}$ initialized from $1/k$. We set $M = 10,000$ (which can be parallel evaluated) and a relatively small k (e.g., $k \leq 15$).

Although the optimization in (4) is equivalent to that of (2), it is equipped with an over-parameterized and more natural coordinate and better initialization, and hence tends to yield better results when solved with gradient-based optimization methods. In particular, the update of the combination weights $\{w_{(i)}\}$ corresponds to fast and global move in the linear span of the basis vectors $\{\xi_{(i)}^0\}_{i=1}^k$, making it easier to escape local optima.

In practice, as we use BigGAN, the latent code $\xi = (z, y)$ is initialized with $z \sim \mathcal{N}(0, I)$ and y randomly selected from the latent representations for the 1,000 classes of ImageNet (which is better than initializing $y \sim \mathcal{N}(0, I)$ as we show in Appendix).

Gradient-based or Gradient-free Optimizer? In this work, we adopt the widely-used Adam [17] optimizer. Some recent works recommended to use gradient-free optimizers, like BasinCMA [3, 16, 32], for optimizing in GAN spaces due to the high non-convexity. However, our study shows that BasinCMA tends to cast a higher computation cost than Adam, because BasinCMA requires a

Algorithm 1 FuseDream (with single image generation)

- 1: **Input:** Query text \mathcal{T} ; a GAN g ; CLIP $\{f_{\text{text}}, f_{\text{image}}\}$.
 - 2: Generate M initialization $\{\xi_i^0\}_{i=1}^M$ randomly, and select the top- k $\{\xi_{(i)}^0\}_{i=1}^k$ with the highest s_{AugCLIP} .
 - 3: Solve the optimization problem (4) using Adam, with $\{\xi_{(i)}\}_{i=1}^k$ initialized from $\{\xi_{(i)}^0\}_{i=1}^k$.
 - 4: **return** image $\mathcal{I} = g \left(\sum_{i=1}^k w_{(i)} \xi_{(i)} \right)$.
-

Algorithm 2 FuseDream-Composition

- 1: **Input:** Query text \mathcal{T} ; a GAN g ; CLIP $\{f_{\text{text}}, f_{\text{image}}\}$. A finite candidate set Γ of the composition parameter $\bar{\alpha}$.
 - 2: **for** $\bar{\alpha}$ in Γ **do**
 - 3: Solve the optimization problem (5) with (6), yielding a composed image $\mathcal{I}_{\bar{\alpha}}$.
 - 4: **end for**
 - 5: **return** image $\mathcal{I}_{\bar{\alpha}}, \bar{\alpha} \in \Gamma$ with the highest s_{AugCLIP} .
-

large number of forward passes on the objective at each iteration, while Adam only requires a single forward and backward pass. Empirically, we found that Adam is $\times 20$ faster than BasinCMA. Although gradient-based methods are more prone to local optima than gradient-free methods, it becomes less an issue with our s_{AugCLIP} loss and the proposed initialization and over-parameterization technique. We include more discussion and comparison with BasinCMA in Appendix.

3.3. Composed generation

The space of images of the CLIP+GAN approach is limited by the representation power of the GAN we use. This makes the method difficult to generate out-of-distribution images and prone to inherit the data biases e.g., center, spatial and color bias [2, 16], from the original training set of the GAN. We propose *composed generation*, which expands the image space and reduce the data bias by composing two images generated by GAN to gain highly flexibility.

Our method co-optimizes a foreground image $\mathcal{I}_{fg} = g(\bar{\xi}_{fg})$ and a background image $\mathcal{I}_{bg} = g(\bar{\xi}_{bg})$, where $\bar{\xi}_{fg}$ and $\bar{\xi}_{bg}$ are two over-parameterized latent codes as Eq 4. The two images are used to generate a fused image

$$\mathcal{I}_{\text{Fuse}} = \text{Fuse}(\mathcal{I}_{fg}, \mathcal{I}_{bg}, \{\alpha, t\})$$

by first scaling \mathcal{I}_{fg} in size with a factor $\alpha \in (0, 1)$, and then pasting it on top of \mathcal{I}_{bg} at one of 9 locations $t \in \{\text{left}, \text{center}, \text{right}\}^2$. We hope to choose $\bar{\xi} := \{\bar{\xi}_{fg}, \bar{\xi}_{bg}\}$, and $\bar{\alpha} := \{\alpha, t\}$ to maximize the s_{AugCLIP} score of \mathcal{I} :

$$s_{\text{Fuse}}(\bar{\xi}, \bar{\alpha}) := s_{\text{AugCLIP}}(\mathcal{T}, \mathcal{I}_{\text{Fuse}}).$$

On the other hand, because the two images \mathcal{I}_{fg} and \mathcal{I}_{bg} are generated independently, the composed image may have

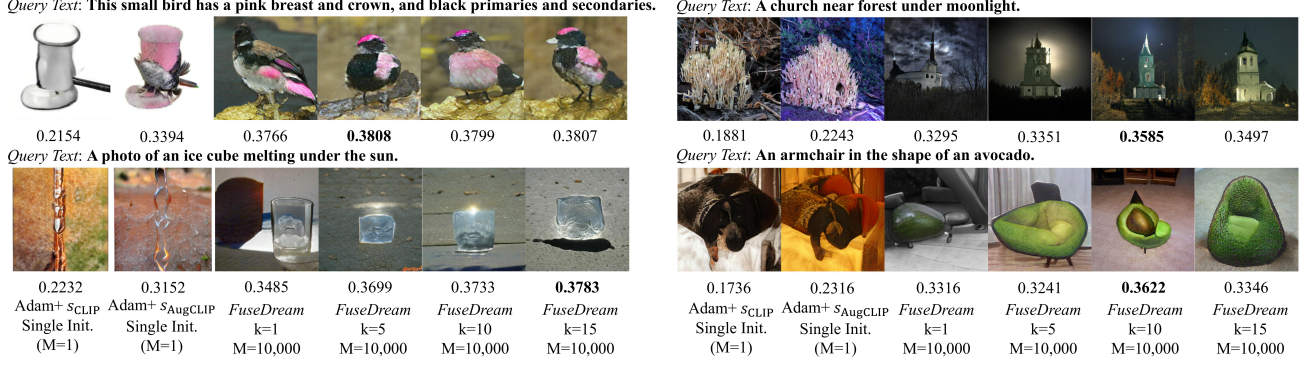


Figure 4. Ablation of different initialization and optimization strategies (Init.=Initialization). The numbers below the images are the s_{AugCLIP} score. \mathbf{z} is randomly initialized from the standard Gaussian distribution and \mathbf{y} is initialized from the latent representations from the 1,000 classes in ImageNet. The left top query text is from the CUB dataset [34]. We can see that: (1) images with higher s_{AugCLIP} tend to interpret the input text better, indicating the effectiveness of s_{AugCLIP} ; (2) *FuseDream* (right three columns of each panel) with $M = 10,000$ and large k generates high s_{AugCLIP} and high-quality images with multiple mixed concepts and nonexistent objects.

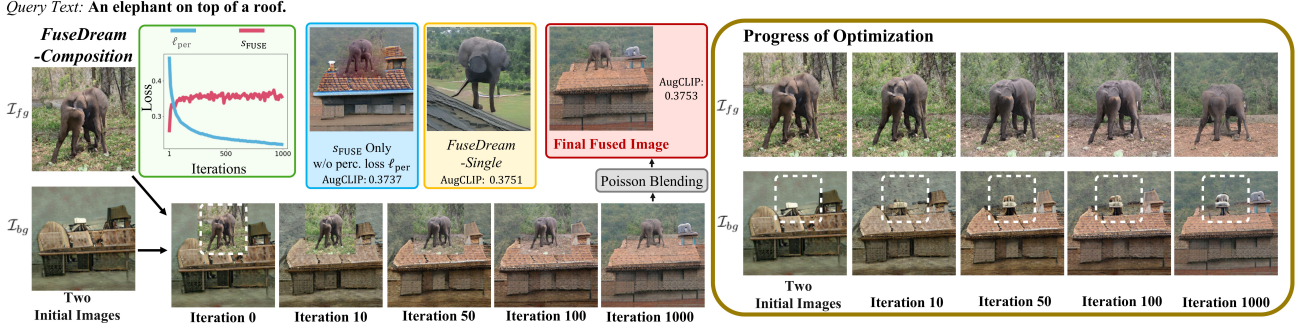


Figure 5. Red box: Image generated by *FuseDream-Composition* on ‘An elephant on top of a roof’. Blue box: Image given by composed generation that only optimizes the s_{FUSE} without considering the perceptual loss ℓ_{FUSE} , which shows a clear discontinuity between \mathcal{I}_{bg} and \mathcal{I}_{fg} . Yellow box: Image given by *FuseDream* without composition, which has a less clear elephant without nose and unrecognizable ‘roof’, because BigGAN cannot handle composed concepts well. Green Box: The AugCLIP score s_{FUSE} and perceptual loss ℓ_{FUSE} vs. iteration using the algorithm in (6). Note that the generated images in blue and red boxes have similar AugCLIP, indicating that the bi-level optimization can improve ℓ_{FUSE} for free without sacrificing s_{FUSE} . The white dashed box on \mathcal{I}_{bg} indicates the position and size of \mathcal{I}_{fg} . Notice how the style and the color of \mathcal{I}_{fg} and \mathcal{P}_{bg} slowly unify across the iteration.

unnatural and artificial discontinuity on the boundary. To address this, we introduce an additional loss that enforces the perceptual consistency between \mathcal{I}_{fg} and \mathcal{I}_{bg} ,

$$\ell_{\text{FUSE}}(\bar{\xi}, \bar{\alpha}) := \ell_{\text{per}}(\mathcal{I}_{fg}, \text{Crop}(\mathcal{I}_{bg}, \{\alpha, t\})),$$

where ℓ_{per} denotes the LPIPS metric [37], a measure that approximates human perception of image similarity.

Hence, we want to both maximize the s_{FUSE} and minimize the perceptual loss ℓ_{FUSE} . A naive approach is to optimize their linear combination. However, this would require a careful and case-by-case tuning of the combination coefficient when generating each image.

Bi-level Optimization We propose a *tuning-free* approach for combining two losses via a simple bi-level (or lexicographic) optimization problem (see e.g., [8, 12]),

$$\min_{\bar{\xi}, \bar{\alpha}} \ell_{\text{FUSE}}(\bar{\xi}, \bar{\alpha}) \quad \text{s.t.} \quad (\bar{\xi}, \bar{\alpha}) \in \arg \max s_{\text{FUSE}}, \quad (5)$$

where $\arg \max s_{\text{FUSE}}$ denotes the set of (local) maxima of s_{FUSE} . This formulation seeks in the optimum set of s_{FUSE} the points that minimize ℓ_{FUSE} . It prioritizes the optimization of s_{FUSE} while incorporating ℓ_{FUSE} as a secondary loss.

We optimize $\bar{\alpha} = \{\alpha, t\}$ by brute-force search in the discrete set $\alpha \in \{0.65, 0.5\}$ and $t \in \{\text{left}, \text{center}, \text{right}\}^2$. For each fixed $\bar{\alpha}$, we optimize the continuous vector $\bar{\xi}$ using the dynamic barrier gradient descent algorithm from [12], which yields the following simple update rule at iteration t ,

$$\begin{aligned} \bar{\xi}^{t+1} &\leftarrow \bar{\xi}^t - \epsilon^t \mathbf{v}^t, \quad \mathbf{v}^t = \nabla \ell_{\text{FUSE}}^t - \lambda_t \nabla s_{\text{FUSE}}^t, \\ \lambda_t &= \max \left(\frac{\beta \|\nabla s_{\text{FUSE}}^t\|^2 + \langle \nabla \ell_{\text{FUSE}}^t, \nabla s_{\text{FUSE}}^t \rangle}{\|\nabla s_{\text{FUSE}}^t\|^2}, 0 \right), \end{aligned} \quad (6)$$

where $\epsilon^t > 0$ is the step size; β is a hyperparameter ($\beta = 1$ by default); we wrote that $\nabla s_{\text{FUSE}}^t = \nabla_{\bar{\xi}} s_{\text{FUSE}}(\bar{\xi}^t)$ and $\nabla \ell_{\text{FUSE}}^t = \nabla_{\bar{\xi}} \ell_{\text{FUSE}}(\bar{\xi}^t)$.

Intuitively, one may view this algorithm as iteratively minimizing the linearly combined loss $\ell_{\text{Fuse}} - \lambda_t s_{\text{Fuse}}$, with the coefficient λ_t dynamically decided by the angle between gradient $\nabla \ell_{\text{Fuse}}$ and ∇s_{Fuse} , in a way that removes the component of $-\nabla \ell_{\text{Fuse}}$ that is conflict with ∇s_{Fuse} , so that s_{Fuse} is ensured to decrease monotonically given that it is the primary loss. See Appendix and [11] for more details.

In practice, we combine (6) with Adam by treating v^t as the gradient direction. In addition, we obtain the final composed image by applying Poisson blending on \mathcal{I}_{fg} and \mathcal{I}_{bg} to yield even smoother image \mathcal{I} following [16]. Our algorithm is summarized in Alg. 2.

4. Related Works

The general idea of optimizing in the latent space of GAN has been widely used as a powerful framework for generating, editing and recovering images; see, e.g., [1, 14, 16, 39], to name only a few. For example, [39] proposes to project real images to the latent space of GAN to edit images. [14] applied principal component analysis to the GAN space to create interpretable controls for image synthesis. [16] optimizes the latent code to embed a given image into the BigGAN [4] by a gradient-free optimizer, BasinCMA [3, 32], to allow flexible image editing in the GAN space. A recent work [7] uses a layer-wise optimization to improve the performance of solving inverse problems, such as super-resolution and inpainting, with GAN space. Most of these methods solely focus on a single task on the image domain, while our method aims to connect images with text by leveraging the power of CLIP.

On the other direction, the idea of using CLIP score [24] has been explored in various directions, including video retrieval [21], visual question answering [30], and language-guided image manipulation/generation [6, 10, 20, 23]. In particular, [23] adopts CLIP and StyleGAN to guide the style of a simple image, typically a photo of face, pet or car. [6, 10, 20] are open-source repositories that implemented the vanilla GAN+CLIP procedure, which we improves substantially with the new techniques.

5. Experiments

We compare *FuseDream* equipped with BigGAN-256 with a number of baselines including DM-GAN [40], Obj-GAN [18], CogView [9], and etc. We test the methods on the popular MS COCO dataset [19], and find that *FuseDream* clearly outperforms baselines even though BigGAN was pretrained on ImageNet. Thanks to the rich representation power brought by CLIP, *FuseDream* can generate images with varying aspects, including artistic style, weather, background, texture, and etc., and is capable of creating nonexistent, counterfactual yet plausible objects. In addition, with the composed generation technique, we can gener-

Methods	IS (↑)	FID (↓)	CLIP R-prec (↑)	R-prec (↑)
Real Images [15]	34.88±0.01	6.09±0.05	82.84±0.04	68.58±0.08
GAN-IC [26]	7.88±0.07	-	-	-
StackGAN [36]	8.45±0.03	-	-	-
AttnGAN [35]	23.79±0.32	28.76	65.66±2.83	82.98±3.15
P-AttnGAN [18]	26.31±0.43	41.51	-	86.71±2.97
Obj-GAN [18]	27.37±0.22	25.85	-	86.20±2.98
DM-GAN [40]	32.32±0.23	27.34±0.11	65.45±2.18	91.87±0.28
OP-GAN [15]	27.88±0.12	24.70±0.09	-	89.01±0.26
DF-GAN [31]	-	21.42	66.42±1.49	-
DALL-E [25]	17.9	27.5	-	-
CogView [9]	18.2	27.1	-	-
BigSleep [20]	13.32 ± 0.45	66.46	91.89±0.31	28.75±3.32
<i>FuseDream</i> (k=5) (256)	34.26 ± 0.76	21.16	96.43±0.24	65.56±1.37
<i>FuseDream</i> (k=10) (256)	34.67 ± 0.97	21.89	98.46±0.17	66.06±0.59
<i>FuseDream</i> (k=5) (512)	34.19±0.95	21.52	98.38±0.18	63.67±1.90
<i>FuseDream</i> (k=10) (512)	32.88±0.93	25.24	98.44±0.15	63.80±1.12

Table 1. Comparison with state-of-the-art text-to-image generators on the test set of MS COCO. Our method gets the highest Inception Score and the lowest FID score. Note that the text-to-image GANs in the second block are directly trained on COCO to maximize the retrieval performance of the model in [35] during training, and hence have much higher R-precision even than the real images. For fair comparison, we also report R-precision calculated by the CLIP model.

erate better images with multiple objects. See Appendix for high resolution copies of the images shown in the paper.

Quantitative Evaluation on MS COCO Test Set To compare with other text-to-image generation methods, we evaluate our methods on a subset of 30,000 captions sampled from the COCO dataset. We follow the same standard evaluation protocol in [18, 31, 35, 40], with the official code provided by [18]². We use Fréchet inception distance (FID), Inception score (IS) and R-precision to evaluate the performance. For R-precision, following [18, 31, 35, 40], we compute the cosine similarity between a global image vector and 100 candidate sentence vectors, extracted by a pre-trained CNN-RNN retrieval model [35]. The candidate text descriptions include one ground-truth caption and 99 randomly selected unrelated sentences. R-precision is computed as the retrieval accuracy of all the 30,000 generated images. We randomly repeat the process for 3 times and report the mean and the standard deviation of R-precision. Note that baseline GANs are usually trained to maximize this score. For fair comparison, we replace the retrieval model used in [35] with the CLIP text and image encoder, and report an additional CLIP R-precision score.

The results are shown in Table 1. *FuseDream* achieves a comparable IS score to that of real images (34.26 versus 34.88). Compared with DALL-E [25] and CogView [9], which are trained on billions of internet images with huge computation cost, we significantly improve the IS score from around 18 to 34, FID from 27 to 21 (e.g. FID 21.16 for *FuseDream* with BigGAN-256, $k = 5$). Note that the BigGAN that we use was trained on ImageNet although the evaluation is on COCO images; we can expect to achieve

²<https://github.com/jamesli1618/Obj-GAN>

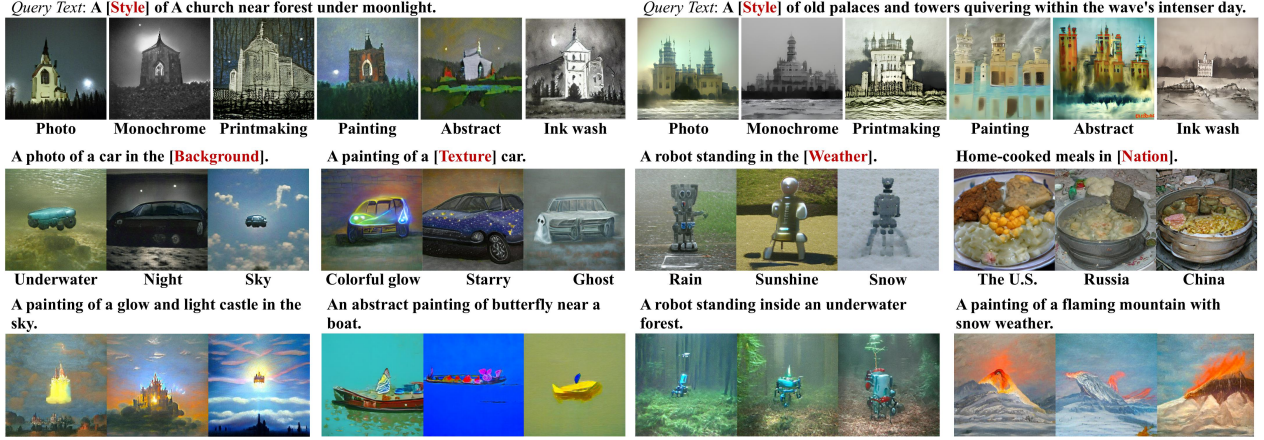


Figure 6. First row: images with different styles generated by our method. Second row: images with different backgrounds, textures, weather, and etc. Third row: more complicated examples combining multiple objects, textures, styles, and other information together. The three images in the third row are selected out of 5 random seeds according to the AugCLIP score.

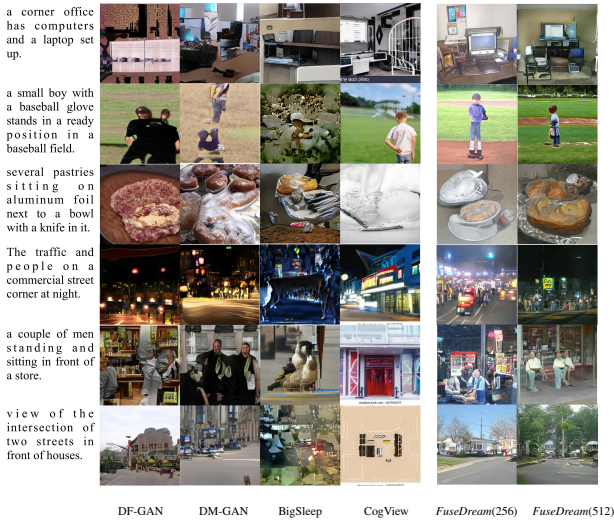


Figure 7. Comparison between *FuseDream* and DF-GAN [31], DM-GAN [40], BigSleep [20], CogView [9] on MS COCO test set. *FuseDream* can handle the complicated captions from MS COCO and generate meaningful images.



Figure 8. Counterfactual images generated by our method. The three images in each panel are selected out of 5 random seeds according to AugCLIP value.

better results by using a stronger generative model trained on COCO dataset.

Images Generated From COCO Captions We show a number of generated images given input captions from COCO dataset in Figure 7. *FuseDream* generates images with more details and objectives. For example, given ‘*The traffic and people on a commercial street corner at night*’, *FuseDream* can generate people, cars and a prosperous street with many lights.

Varying Artistic Styles Although BigGAN is trained on the ImageNet whose images are mostly realistic, with CLIP, *FuseDream* is capable of producing meaningful images with different artistic styles, as displayed in the first row in Figure 6. The images are with six different styles, e.g. photo, monochrome, printmaking, painting, abstract painting and ink and wash painting. We can generate meaningful fake images with *many granularities* even if the input sentence is complicated. Given the sentence (‘*old palaces and towers quivering within the wave’s intenser day*’) from Percy Shelley’s *Ode to the West Wind*, *FuseDream* successfully generates palaces, towers, wave, and day light.

Varying Textures, Backgrounds and More As shown in [14, 29], it is hard to control texture and background in standard GANs. However, *FuseDream* can nicely control the texture and background of images through the input sentences. As shown in the second and third rows of Figure 6, *FuseDream* easily put a car in different backgrounds (e.g. *underwater*, *night*, *sky*) and with different textures (e.g. *colorful glow*, *starry*, *ghost*). Changing the object to robot, we can also generate meaningful but fake robots under different weather (e.g. *rain*, *sunshine*, *snow*). Moreover, *FuseDream* seems to show understanding about cultural difference by generating obviously different meals for the U.S., Russia and China: meal of *the U.S.* contains

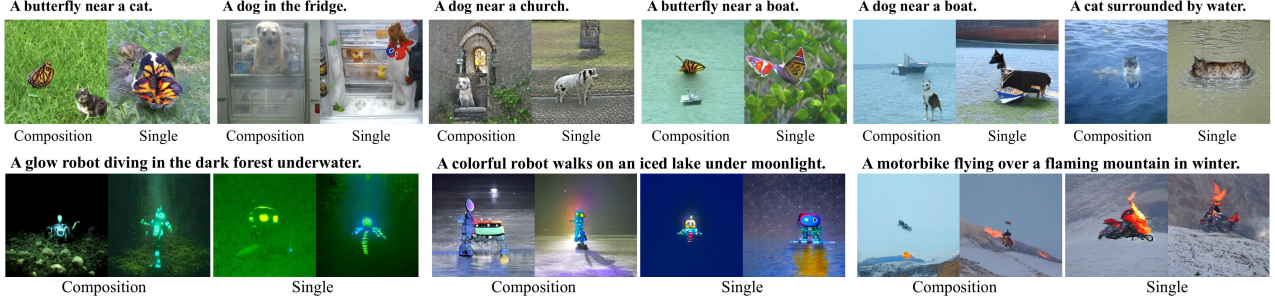


Figure 9. Images from *FuseDream* (with single image generation) and *FuseDream-Composition*. We find that: (1) *FuseDream-Composition* can generate seamlessly fused images with no unnatural discontinuous on the fusing boundary; (2) Prompted with the simple query texts in the top row, *FuseDream* (single) tends to mix two objects together or ignore some concepts in the query, while *FuseDream-Composition* can generate images with clear and disentangled objects; (3) For the more complex text in the second row, *FuseDream-Composition* can generate images with fine-grained details (e.g., ‘dark forest’, ‘walk’, ‘moonlight’, ‘flying’, ‘flaming mountain’).



Figure 10. More mages generated by *FuseDream-Composition* for ‘A colorful robot walks on an iced lake under moonlight’, verifying that our method can generate high-quality images with different random seeds. The 36 images are selected out of 50 random seeds according to the AugCLIP score, and are ordered with descending AugCLIP score (from the left to right, the top to down).

corn, potato mesh and fried chicken; meal of *Russia* contains black bread and Russian Borscht; meal of *China* contains egg dumplings and spring rolls.

Generating Counterfactual Contents In previous examples, we have shown some counterfactual examples, e.g. flaming dogs in Figure 1, car in the sky in Figure 6. Here, we use *FuseDream* to generate more high-quality counterfactual images with different objects, background and style.

Figure 8 demonstrates that we can generate ‘glow and light dog’, ‘castle in the sky’, ‘cube butterfly’ and ‘underwater forest’. These images have different objects, backgrounds and styles, and do not appear in real world, nor in BigGAN’s ImageNet training data. It is surprising that *FuseDream* successfully generates these out-of-domain images with high quality, especially given that we never change the parameters of the BigGAN.

Multiple Concepts with *FuseDream-Composition*: We verify the performance of composed generation technique by generating images that contain two objects. These two objects do not typically co-appear in normal images, e.g. cat and butterfly, dog and church, etc. As shown in Figure 9, *FuseDream* (with single image generation) may entangle the two objects together or miss one of the objects.

For example, ‘a dog near a boat’ gives a boat with a dog-like sail. ‘A butterfly near a boat’ generates only a butterfly while missing the boat. However, by using composed generation, we can generate images with both objects. Even for more complicated sentences, we can generate meaningful and high-quality images (see the second row in Figure 9).

To verify the robustness of our method to random seed, we generate more images in Figure 10 for ‘A colorful robot walks on an iced lake under moonlight’; we obtain a diverse set of images that are well related to the sentence.

6. Conclusions

We propose *FuseDream*, which enables high quality, state-of-the-art text-to-image generation with CLIP-guided GAN. Compared with traditional training-based approaches, our method is training-free, zero-shot, easily customizable, and is hence easily accessible to users with limited computational resource or special demands. Our novel techniques of AugCLIP score, over-parameterized optimization and composed generation are of independent interest and useful in other latent space optimization problems.

References

- [1] Rameen Abdal, Yipeng Qin, and Peter Wonka. Image2stylegan: How to embed images into the stylegan latent space? In *Proceedings of the IEEE/CVF International Conference on Computer Vision*, pages 4432–4441, 2019. 2, 6
- [2] Rushil Anirudh, Jayaraman J Thiagarajan, Bhavya Kailkhura, and Timo Bremer. Mimicgan: Robust projection onto image manifolds with corruption mimicking. *arXiv preprint arXiv:1912.07748*, 2019. 4
- [3] David Bau, Jun-Yan Zhu, Jonas Wulff, William Peebles, Hendrik Strobelt, Bolei Zhou, and Antonio Torralba. Seeing what a gan cannot generate. In *Proceedings of the IEEE/CVF International Conference on Computer Vision*, pages 4502–4511, 2019. 4, 6, 12
- [4] Andrew Brock, Jeff Donahue, and Karen Simonyan. Large scale gan training for high fidelity natural image synthesis. In *International Conference on Learning Representations*, 2018. 2, 3, 6
- [5] Jeremy Cohen, Elan Rosenfeld, and Zico Kolter. Certified adversarial robustness via randomized smoothing. In *International Conference on Machine Learning*, pages 1310–1320. PMLR, 2019. 4
- [6] Katherine Crowson. Vqgan + clip. <https://github.com/nerdyrodent/VQGAN-CLIP>. 2, 6
- [7] Giannis Daras, Joseph Dean, Ajil Jalal, and Alexandros G Dimakis. Intermediate layer optimization for inverse problems using deep generative models. *arXiv preprint arXiv:2102.07364*, 2021. 6
- [8] Stephan Dempe and Alain Zemkoho. *Bilevel optimization*. Springer, 2020. 5
- [9] Ming Ding, Zhuoyi Yang, Wenyi Hong, Wendi Zheng, Chang Zhou, Da Yin, Junyang Lin, Xu Zou, Zhou Shao, Hongxia Yang, et al. Cogview: Mastering text-to-image generation via transformers. *arXiv preprint arXiv:2105.13290*, 2021. 1, 6, 7
- [10] Federico A Galatolo, Mario GCA Cimino, and Gigliola Vaglini. Generating images from caption and vice versa via clip-guided generative latent space search. *arXiv preprint arXiv:2102.01645*, 2021. 2, 6
- [11] Chengyue Gong, Xingchao Liu, et al. Automatic and harmless regularization with constrained and lexicographic optimization: A dynamic barrier approach. In *Thirty-Fifth Conference on Neural Information Processing Systems*, 2021. 2, 6
- [12] Chengyue Gong, Xingchao Liu, and Qiang Liu. Bi-objective trade-off with dynamic barrier gradient descent. *Advances in neural information processing systems*, 2021. 5
- [13] Ian J Goodfellow, Jonathon Shlens, and Christian Szegedy. Explaining and harnessing adversarial examples. *arXiv preprint arXiv:1412.6572*, 2014. 3
- [14] Erik Härkönen, Aaron Hertzmann, Jaakko Lehtinen, and Sylvain Paris. Ganspace: Discovering interpretable gan controls. *arXiv preprint arXiv:2004.02546*, 2020. 6, 7
- [15] Tobias Hinz, Stefan Heinrich, and Stefan Wermter. Semantic object accuracy for generative text-to-image synthesis. *IEEE transactions on pattern analysis and machine intelligence*. 6
- [16] Minyoung Huh, Richard Zhang, Jun-Yan Zhu, Sylvain Paris, and Aaron Hertzmann. Transforming and projecting images into class-conditional generative networks. In *European Conference on Computer Vision*, pages 17–34. Springer, 2020. 3, 4, 6, 12
- [17] Diederik P Kingma and Jimmy Ba. Adam: A method for stochastic optimization. In *ICLR (Poster)*, 2015. 2, 3, 4
- [18] Wenbo Li, Pengchuan Zhang, Lei Zhang, Qiuyuan Huang, Xiaodong He, Siwei Lyu, and Jianfeng Gao. Object-driven text-to-image synthesis via adversarial training. In *Proceedings of the IEEE/CVF Conference on Computer Vision and Pattern Recognition*, pages 12174–12182, 2019. 1, 2, 6
- [19] Tsung-Yi Lin, Michael Maire, Serge Belongie, James Hays, Pietro Perona, Deva Ramanan, Piotr Dollár, and C Lawrence Zitnick. Microsoft coco: Common objects in context. In *European conference on computer vision*, pages 740–755. Springer, 2014. 2, 6
- [20] Lucidrains. Big sleep. <https://github.com/lucidrains/big-sleep>. 1, 2, 3, 6, 7
- [21] Huaishao Luo, Lei Ji, Ming Zhong, Yang Chen, Wen Lei, Nan Duan, and Tianrui Li. Clip4clip: An empirical study of clip for end to end video clip retrieval. *arXiv preprint arXiv:2104.08860*, 2021. 6
- [22] Elman Mansimov, Emilio Parisotto, Jimmy Lei Ba, and Ruslan Salakhutdinov. Generating images from captions with attention. *arXiv preprint arXiv:1511.02793*, 2015. 1
- [23] Or Patashnik, Zongze Wu, Eli Shechtman, Daniel Cohen-Or, and Dani Lischinski. Styleclip: Text-driven manipulation of stylegan imagery. In *Proceedings of the IEEE/CVF International Conference on Computer Vision*, pages 2085–2094, 2021. 6
- [24] Alec Radford, Jong Wook Kim, Chris Hallacy, Aditya Ramesh, Gabriel Goh, Sandhini Agarwal, Girish Sastry, Amanda Askell, Pamela Mishkin, Jack Clark, et al. Learning transferable visual models from natural language supervision. *arXiv preprint arXiv:2103.00020*, 2021. 2, 6
- [25] Aditya Ramesh, Mikhail Pavlov, Gabriel Goh, Scott Gray, Chelsea Voss, Alec Radford, Mark Chen, and Ilya Sutskever. Zero-shot text-to-image generation. *arXiv preprint arXiv:2102.12092*, 2021. 1, 6
- [26] Scott Reed, Zeynep Akata, Xinchun Yan, Lajanugen Logeswaran, Bernt Schiele, and Honglak Lee. Generative adversarial text to image synthesis. In *International Conference on Machine Learning*, pages 1060–1069. PMLR, 2016. 1, 6
- [27] Olga Russakovsky, Jia Deng, Hao Su, Jonathan Krause, Sanjeev Satheesh, Sean Ma, Zhiheng Huang, Andrej Karpathy, Aditya Khosla, Michael Bernstein, et al. Imagenet large scale visual recognition challenge. *International journal of computer vision*, 115(3):211–252, 2015. 2
- [28] Hadi Salman, Greg Yang, Jerry Li, Pengchuan Zhang, Huan Zhang, Ilya Razenshteyn, and Sebastien Bubeck. Provably robust deep learning via adversarially trained smoothed classifiers. *arXiv preprint arXiv:1906.04584*, 2019. 4
- [29] Axel Sauer and Andreas Geiger. Counterfactual generative networks. *arXiv preprint arXiv:2101.06046*, 2021. 7
- [30] Sheng Shen, Liunian Harold Li, Hao Tan, Mohit Bansal, Anna Rohrbach, Kai-Wei Chang, Zhewei Yao, and Kurt

- Keutzer. How much can clip benefit vision-and-language tasks? *arXiv preprint arXiv:2107.06383*, 2021. 6
- [31] Ming Tao, Hao Tang, Songsong Wu, Nicu Sebe, Xiao-Yuan Jing, Fei Wu, and Bingkun Bao. Df-gan: Deep fusion generative adversarial networks for text-to-image synthesis. *arXiv preprint arXiv:2008.05865*, 2020. 1, 6, 7
- [32] Kevin Wampler and Zoran Popović. Optimal gait and form for animal locomotion. *ACM Transactions on Graphics (TOG)*, 28(3):1–8, 2009. 4, 6, 12, 17
- [33] Xintao Wang, Liangbin Xie, Chao Dong, and Ying Shan. Real-esrgan: Training real-world blind super-resolution with pure synthetic data. In *International Conference on Computer Vision Workshops (ICCVW)*. 12, 18
- [34] Peter Welinder, Steve Branson, Takeshi Mita, Catherine Wah, Florian Schroff, Serge Belongie, and Pietro Perona. Caltech-ucsd birds 200. 2010. 5
- [35] Tao Xu, Pengchuan Zhang, Qiuyuan Huang, Han Zhang, Zhe Gan, Xiaolei Huang, and Xiaodong He. Attngan: Fine-grained text to image generation with attentional generative adversarial networks. In *Proceedings of the IEEE conference on computer vision and pattern recognition*, pages 1316–1324, 2018. 1, 6
- [36] Han Zhang, Tao Xu, Hongsheng Li, Shaoting Zhang, Xiaogang Wang, Xiaolei Huang, and Dimitris N Metaxas. Stackgan: Text to photo-realistic image synthesis with stacked generative adversarial networks. In *Proceedings of the IEEE international conference on computer vision*, pages 5907–5915, 2017. 6
- [37] Richard Zhang, Phillip Isola, Alexei A Efros, Eli Shechtman, and Oliver Wang. The unreasonable effectiveness of deep features as a perceptual metric. In *Proceedings of the IEEE conference on computer vision and pattern recognition*, pages 586–595, 2018. 5
- [38] Shengyu Zhao, Zhijian Liu, Ji Lin, Jun-Yan Zhu, and Song Han. Differentiable augmentation for data-efficient gan training. *arXiv preprint arXiv:2006.10738*, 2020. 3
- [39] Jun-Yan Zhu, Philipp Krähenbühl, Eli Shechtman, and Alexei A Efros. Generative visual manipulation on the natural image manifold. In *European conference on computer vision*, pages 597–613. Springer, 2016. 3, 6
- [40] Minfeng Zhu, Pingbo Pan, Wei Chen, and Yi Yang. Dm-gan: Dynamic memory generative adversarial networks for text-to-image synthesis. In *Proceedings of the IEEE/CVF Conference on Computer Vision and Pattern Recognition*, pages 5802–5810, 2019. 2, 6, 7

A. Implementation Details

We use the official pre-trained BigGAN model in PyTorch³. For initialization, we use $M = 10,000$, where the batch size is 10 and the initialization runs for 1,000 steps. For optimization, we use Adam optimizer with a learning rate of 5×10^{-3} with no weight decay, and optimize for 1,000 iterations. On a GTX 3090 GPU, using BigGAN-256, *FuseDream* approximately requires 100 seconds for initialization and 80 seconds for optimization, resulting in 180 seconds (~ 3 minutes) in total. Changing the pre-trained model to BigGAN-512 increases the initialization time to 220 seconds and the optimization time to 120 seconds (yielding ~ 7 minutes in total).

B. More Studies on Composed Generation

We discuss the design choices for the composed generation in Sec. 3.3. To demonstrate the effectiveness of the bi-level optimization, formulation (5), we consider two alternative formulations for trading off the AugCLIP score s_{Fuse} and the perceptual loss ℓ_{Fuse} of the fused image:

Linear Combination A standard way to trade-off two loss functions is to optimize their linear combination:

$$\min_{\bar{\xi}, \bar{\alpha}} (1 - \lambda)\ell_{\text{Fuse}}(\bar{\xi}, \bar{\alpha}) - \lambda s_{\text{Fuse}}(\bar{\xi}, \bar{\alpha}), \quad (7)$$

where $\lambda \in (0, 1)$ is a linear combination coefficient used to balance the two objectives. However, as shown in Figure 11, the key disadvantage of this approach is that the optimal choice of λ depends on the query text, and hence needs to be tuned by the user case by case. This makes the overall procedure computationally expensive and difficult to automatize. In comparison, the bi-level optimization approach does not require to tune λ case by case, and provides high quality fused image with only a single run.

Inverse Bi-level Optimization In the bi-level optimization in (5), we prioritize the optimization of the AugCLIP score s_{Fuse} while adding the perceptual loss ℓ_{Fuse} as the secondary loss. An alternative approach is to switch the roles of the two loss functions, prioritizing ℓ_{Fuse} and treating s_{Fuse} as the secondary loss:

$$\max_{\bar{\xi}, \bar{\alpha}} s_{\text{Fuse}}(\bar{\xi}, \bar{\alpha}) \quad s.t. \quad (\bar{\xi}, \bar{\alpha}) \in \arg \min \ell_{\text{Fuse}}(\bar{\xi}, \bar{\alpha}). \quad (8)$$

As shown in Figure. 11, this approach does not work as well as (5), because it tends to generate images with poor AugCLIP score. Intuitively, (5) is better because s_{Fuse} is difficult to optimize and ℓ_{Fuse} is much easier to optimize, and hence it makes more sense to prioritize the optimization of s_{Fuse} .

C. Additional Experimental Results

Choice of Initialization As we discussed in Section 3.2, it is recommended to initialize the class label y by randomly selecting from the latent representations for the 1,000 classes of ImageNet. An alternative approach is to initialize y from the standard Gaussian distribution, which, however, leads to highly noisy images as we show in Figure. 12.

Linear Interpolation We linearly interpolate between two generated images to examine the intermediate images in the latent space. Specifically, given two query text \mathcal{T}_1 and \mathcal{T}_2 , and let ξ_1 and ξ_2 be the latent code provided by FuseDream (without composed generation), we generate a sequence of images via

$$\mathcal{I}_\alpha = g(\alpha \xi_1 + (1 - \alpha) \xi_2),$$

where $\alpha \in [0, 1]$. As shown in Figure. 14, the intermediate images provides a smooth interpolation between the images of the two queries.

Influence of the Data Augmentation Techniques We perform an ablation study on choice of data augmentation techniques (random colorization, random translation, random resize, and random cutout) in the AugCLIP score. Results are shown in Figure. 15.

³<https://github.com/ajbrock/BigGAN-PyTorch>

Out-of-domain Generation We use query texts including famous landmarks, arts, animation figures, etc., to examine the ability of *FuseDream* to generate images outside the training domain of ImageNet. As shown in Figure. 15, *FuseDream* can generate famous landmarks, masterpieces, emojis, cartoon characters that are not included in the ImageNet training data.

Optimization with Gradient-free Optimizer We replace Adam and optimize AugCLIP score with BasinCMA optimizer [32], which is a gradient-free optimizer used in previous works [3, 16] for optimizing in the GAN latent space. Results are shown in Figure. 17.

High-resolution images We use [33] to get high-resolution version of sampled generated images in Figure 18.

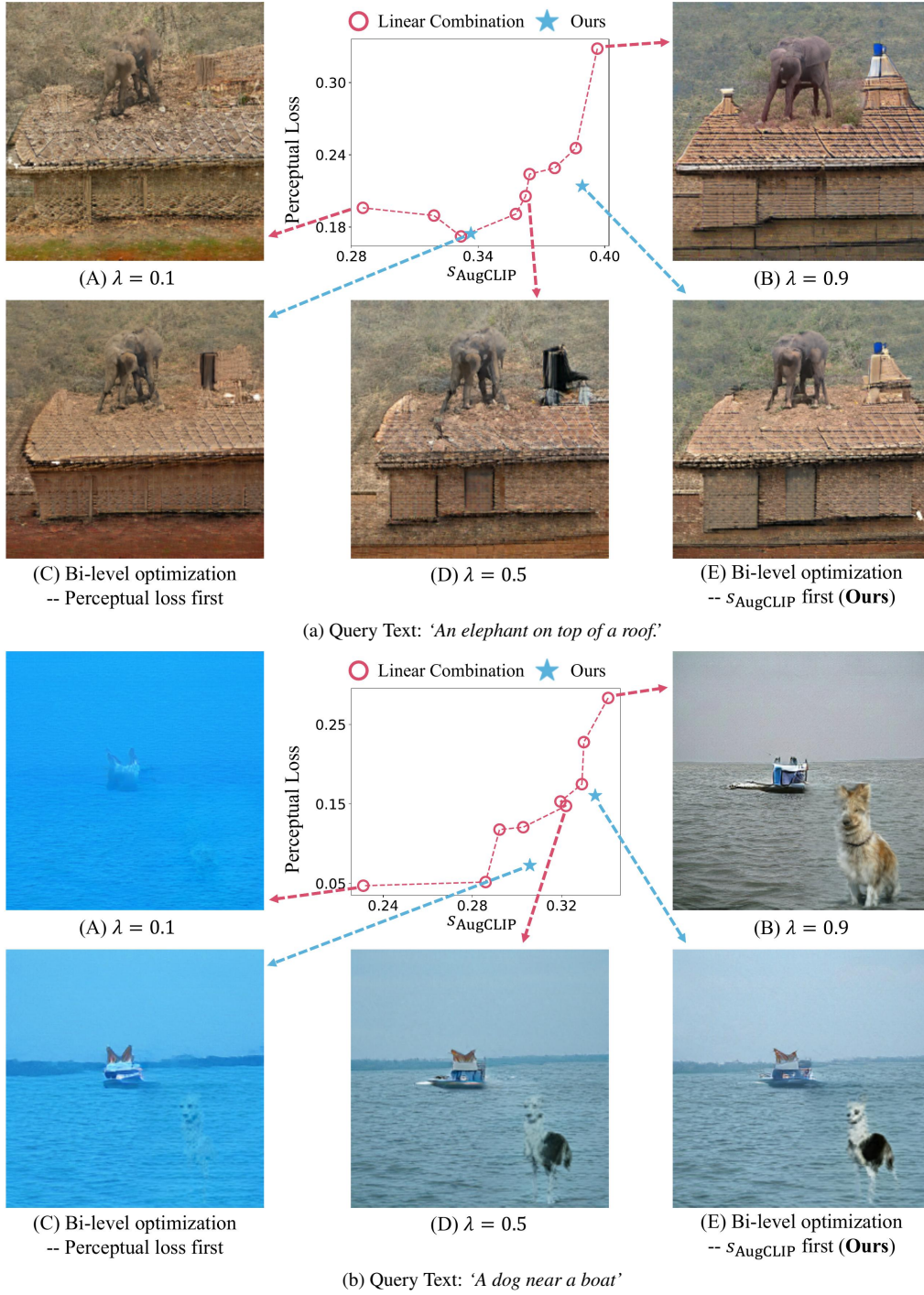


Figure 11. We show two examples to demonstrate the benefit of using our bi-level optimization formulation in composed generation. We compare our formulation (5) with the inverse bi-level optimization (8) and linear combination method (7). We search the linear combination coefficient λ from 0.1 to 0.9 uniformly. Observations: (1) For the linear combination method, For two text queries (a) and (b), the effect of similar λ is different. For instance, when $\lambda = 0.5$, the generated image for (a) has acceptable visual quality, but the generated image for (b) failed to generate recognizable 'dog'; (2) Instead, our bi-level optimization formulation (5) with dynamic-barrier gradient descent relieves the user from tuning λ for each image. It yields low perceptual loss without sacrificing too much of the s_{AugCLIP} score, and finally generates natural fused images; (3) The inverse bi-level optimization (8) formulation cannot get good results.

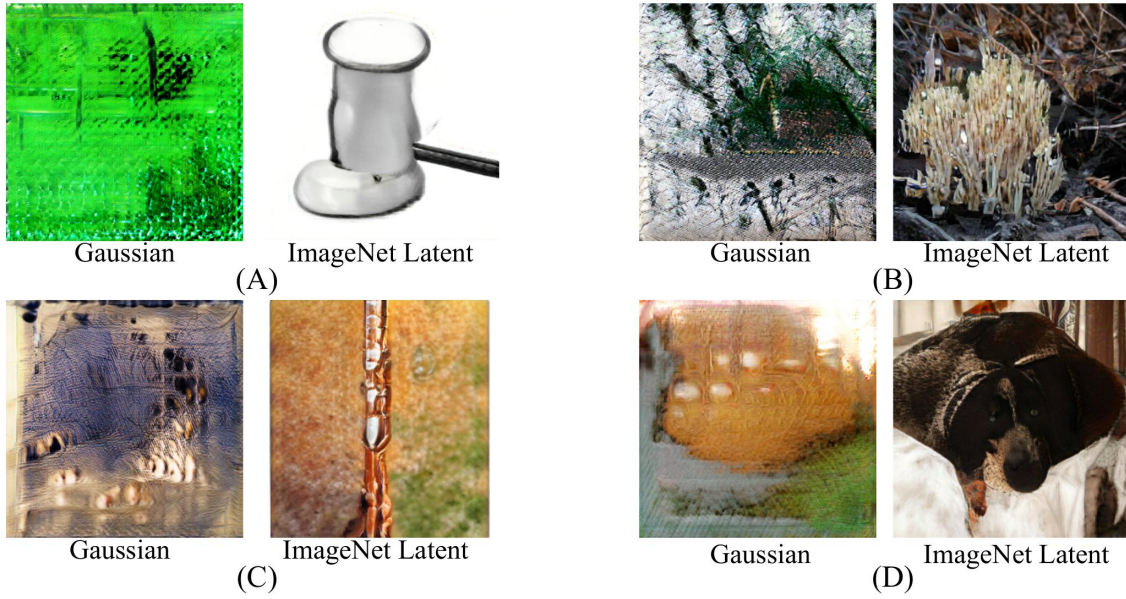


Figure 12. This figures show the other initialization choice (initialize \mathbf{z} and \mathbf{y} from the standard Gaussian distribution $\mathcal{N}(0, I)$) for generating the images in Figure. 4, as mentioned in the main text. After optimization, the generated images are still noises. In comparison, initializing from the latent codes of ImageNet classes gives more natural images. The corresponding query texts are: (A) This small bird has a pink breast and crown, and black primaries and secondaries. (B) A church near forest under moonlight. (C) A photo of an ice cube melting under the sun. (D) An armchair in the shape of an avocado.

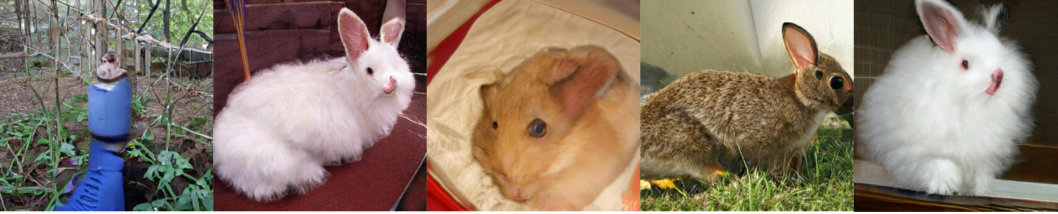


Figure 13. Three examples of linearly interpolating between the latent codes of two generated images. We observe a smooth transition and the intermediate results are still natural and realistic.

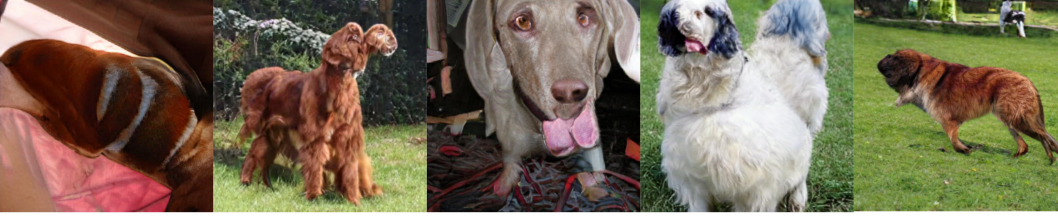
Query Text: **Sunshine in a forest.**



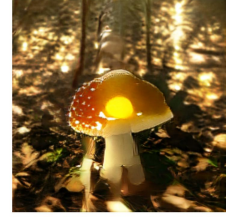
Query Text: **A blue toy rabbit.**



Query Text: **A rainbow dog.**



(A) Initial basis images



(B) Generated Image

Figure 14. The initial basis images when $k = 5$ for the query text ‘Sunshine in a forest’ (top row), ‘A blue toy rabbit’ (middle row) and ‘A rainbow dog’ (bottom row).

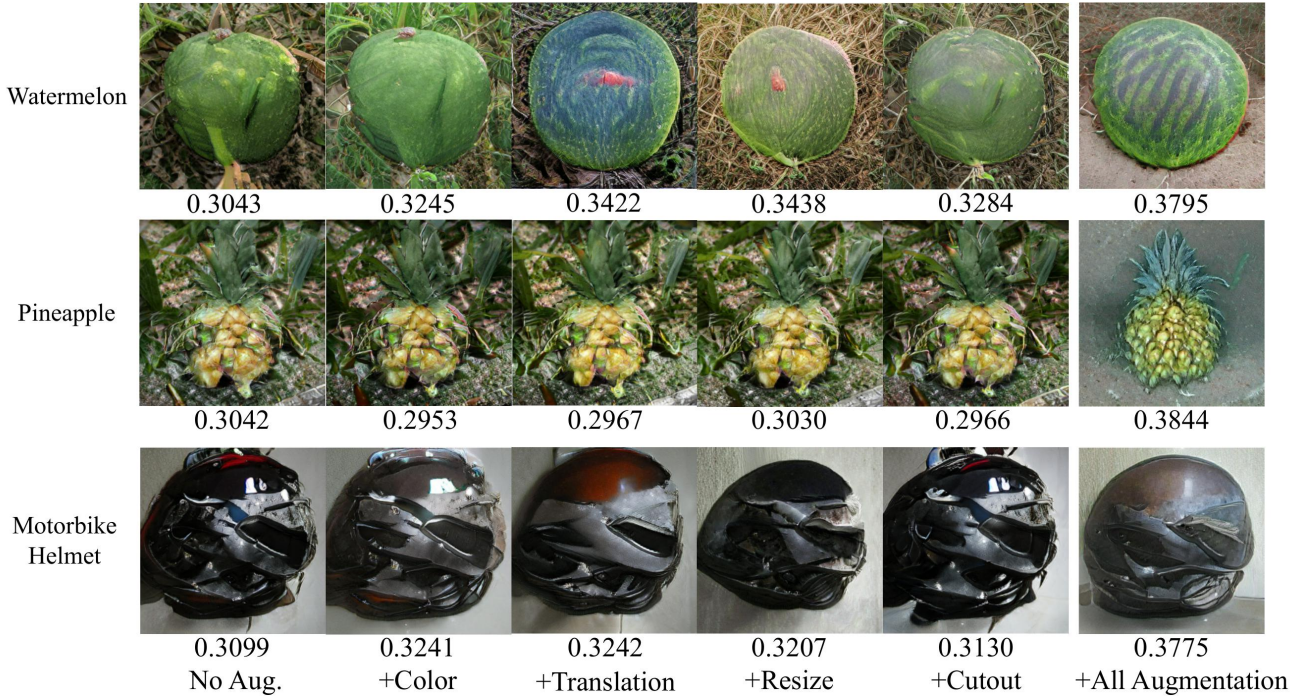
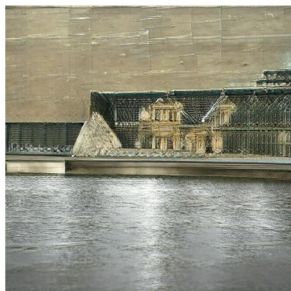


Figure 15. Images generated by *FuseDream* when we incorporate different data augmentation techniques in AugCLIP. The numbers indicate their corresponding AugCLIP score computed with all data augmentation. We observe that each data augmentation technique has their unique influence on the generated image, but the best visual result is obtained by applying all the augmentation techniques.

A photo of the Louvre.



Real

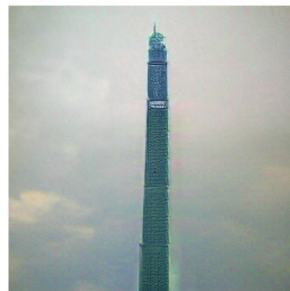


FuseDream

A photo of Taipei 101.



Real



FuseDream

An emoji of a smiling face.

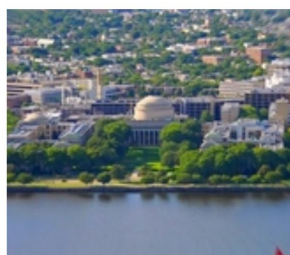


Real

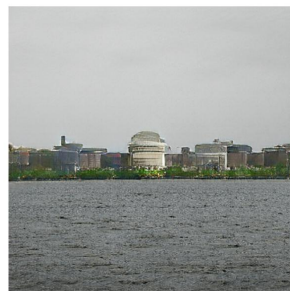


FuseDream

A photo of MIT.



Real



FuseDream

A photo of Pikachu, the Pokemon.



Real



FuseDream

Master Chief from Halo.

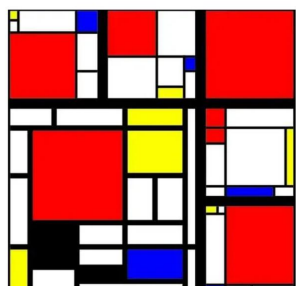


Real

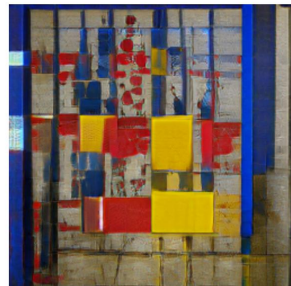


FuseDream

Red, Blue and Yellow by Mondrian.



Real



FuseDream

The painting of Starry night by Van Gogh.



Real



FuseDream

Figure 16. More examples for demonstrating the ability of *FuseDream* to generate images that are outside the training domain (ImageNet) of BigGAN. The ‘real’ images are adopted from the Internet for comparison.



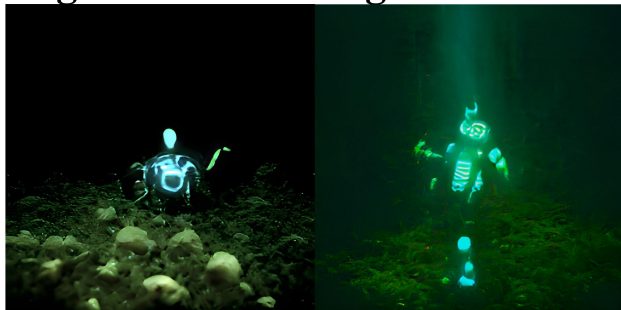
(A) 5 mega-steps (~ 5 minutes)



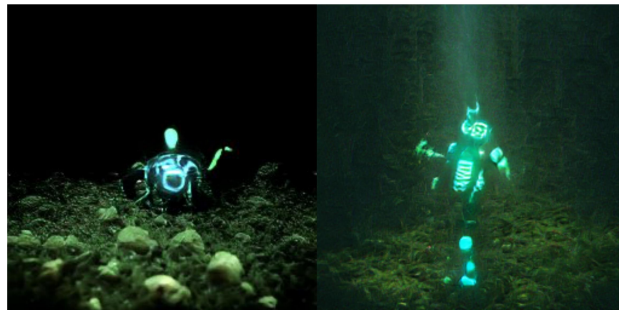
(B) 30 mega-steps (~ 30 minutes)

Figure 17. Direct optimization of the s_{AugCLIP} score with BasinCMA [32] without our proposed initialization and over-parameterization strategy. ‘Mega-step’ refers to the number of iterations in the outer loop when using BasinCMA. We use the same computer with GTX 3090 to test the computational time. The base GAN is BigGAN-256. The objective is s_{AugCLIP} . In Figure.(A), with similar running time (~5 minutes), BasinCMA failed to generate realistic images for ‘pineapple’ and ‘motorbike helmet’, while *FuseDream* successes (See Figure. 15). In Figure.(B), with longer optimization time (~30 minutes), BasinCMA can generate semantically related images.

A glow robot diving in the dark forest underwater.

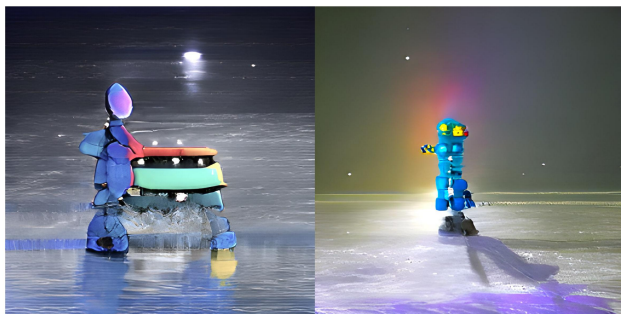


SuperResolution

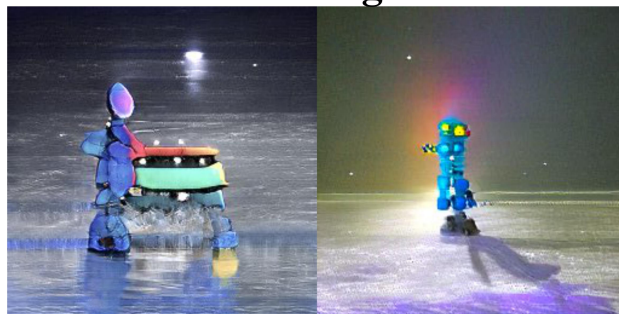


Vanilla

A colorful robot walks on an iced lake under moonlight.



SuperResolution



Vanilla

A motorbike flying over a flaming mountain in winter.



SuperResolution



Vanilla

Figure 18. Original images and their super-resolution version ($\times 4$) generated by [33].